IJCSN International Journal of Computer Science and Network, Volume 5, Issue 4, August 2016
ISSN (Online): 2277-5420 www.IJCSN.org
**Impact Factor: 1.02**



# Exudates Detection of Retinal Images using Otsu's Thresholding and Kirsch's Templates

**[1] Shreyasi Hazra, [2] Atashi Patra , [3] Tuhin Utsab Paul**

[1,2] Student, Electronics and Communication Engineering, Institute of Engineering & Management
Kolkata, West Bengal, India

[3] Asst. Prof., Electronics and Communication Engineering, Institute of Engineering & Management
Kolkata, West Bengal, India

**Abstract - Ophthalmic diseases like diabetic retinopathy, macular degeneration, glaucoma, etc. may cause gradual loss of eyesight and are some of the reasons behind blindness. Hence, blood vessel assessment and segmentation play a key role in the diagnosis of retinal disorders. The manual detection of narrow blood vessels of retinal images is time consuming and may result in erroneous output. Therefore, computer aided, robust and performance oriented algorithm is required to detect and segment the blood vessels efficiently. The present work proposes an algorithm that uses thresholding technique, basic morphological operations and Kirsch's edge detection operator to detect the blood vessels and segment the hard exudates efficiently. The detected exudates regions are then compared with the ground truth exudate regions. Based on the correctly identified exudate regions between these two images, different performance parameters like accuracy, specificity, sensitivity, PPV, PLR and misclassified proportions have been measured to evaluate overall performance of the proposed algorithm. This algorithm successfully detects exudates with an average of 98.47% accuracy, 54.67% sensitivity, 99.82% specificity, 88.62% PPV, 303.73 PLR and 0.17% misclassified proportions.**

**Keywords -** *Retinal Blood Vessel Detection, Kirsch Template, Otsu; Accuracy, Specificity, Sensitivity.*

## 1. Introduction

Image segmentation [1] in the retinal fundus image is the key factor for identification of the retinal blood vessels. The study of the human retina helps the ophthalmologists to recognize the retinal diseases.

Manual method of blood vessel identification and segmentation requires considerable time and the result might be prone to human error. Hence, strong, performance oriented and feature-based algorithm [2] is required for efficient detection of blood vessels.

The images for test purpose are taken from DRIVE [3] and STARE [4] database [5]. The DRIVE database has been established to facilitate quantitative studies on segmentation of blood vessels in retinal images. The DRIVE database contains 40 images, including 20 in test set and 20 in training set. The STARE (STructured Analysis of the Retina) database contains the retinal interior surface picture. Initially, the STARE database was collected by Hoover et al. [6]. The STARE database is used for pathological purpose that contains 20 images [7]. In addition, some of the images have been taken from different eye clinics and image banks' websites.

The acquired images are then pre-processed to make them ready for subsequent processes. After pre-processing, various image processing techniques such as morphological operations, edge detection algorithms, etc. are also used for efficiently extracting the blood vessels and locating the hard exudates regions.

First, a literary survey [8] has been done to perform a comparative study on various performance parameters of few existing works.

In this proposed algorithm, Otsu's algorithm is used for binarization using an appropriate threshold level. Also, Kirsch's template operator has been used for extraction of blood vessels. Once the exudate regions have been detected, the output image is compared with the ground truth exudate regions. Finally, different performance parameters like accuracy, sensitivity, specificity, PPV, PLR and misclassified proportions are measured to evaluate the effectiveness of the proposed algorithm [8].

## 2. Methodology

### 2.1 Adaptive Histogram Equalization

Histogram equalization is the process of altering the image intensity values in a way that the histogram of the output images approximately go with the specified histogram. This method increases the global contrast of the images [9].

However, Contrast Limited Adaptive Histogram Equalization (CLAHE) is an enhancement technique which is responsible for improving the local contrast of an image. It computes few numbers of histograms, each corresponding to different sections of the image and uses them to reconstruct the lightness values of the image. CLAHE operates on a small area in the image. The contrast of each small area is enhanced with histogram equalization [10].

### 2.2 Otsu's Thresholding

The Otsu's thresholding technique is used for the detection of the desired area of an image. The resulting image is thresholded using an automatically selected threshold level [11]. The threshold level is a normalized intensity value which lies in the range [0, 1]. It is chosen to minimize the intra-class variance of the black and white pixels [12].

In the Otsu's method we comprehensively search for the threshold that minimizes the intra-class variance (the variance within the class), defined as a weighted sum of variances of the two classes:

$$\sigma_{\omega}^2(t) = \omega_0(t)\,\sigma_0^2(t) + \omega_1(t)\,\sigma_1^2(t) \quad (1)$$

Weights $\omega_{0,1}$ are the probabilities of the two classes which are separated by a threshold t and $\sigma_{0,1}^2$ are variances of these two classes. The class probability $\omega_{0,1}$ (t) is then computed from the L histograms:

$$\omega_0(t) = \sum_{i=0}^{t-1} p(i) \quad (2)$$

$$\omega_1(t) = \sum_{i=t}^{L-1} p(i) \quad (3)$$

Otsu shows that minimizing the intra-class variance is the same as maximizing inter-class variance which is estimated in terms of class probabilities ω and class means μ: [13]

$$\sigma_b^2(t) = \omega_0(t)\omega_1(t)[\mu_0(t) - \mu_1(t)]^2 \quad (4)$$

Here, the class mean $\mu_{0,1,T}(t)$ is expressed as follows:

$$\mu_0(t) = \sum_{i=0}^{t-1} ip(i)/\omega_0 \quad (5)$$

$$\mu_1(t) = \sum_{i=t}^{L-1} ip(i)/\omega_1 \quad (6)$$

$$\mu_T = \sum_{i=0}^{L-1} ip(i) \quad (7)$$

The class probabilities and class means is computed iteratively. This scheme results in an effective algorithm. The algorithm, thus, sums up to:

i. Compute histogram and probabilities of each intensity level of the image
ii. Set up initial $\omega_i(0)$ and $\mu_i(0)$
iii. Step through all possible thresholds t = 1 to maximum intensity
iv. Update $\omega_i$ and $\mu_i$
v. Compute $\sigma_b^2(t)$
vi. Desired threshold corresponds to the maximum $\sigma_b^2(t)$

### 2.3 Kirsch's Template

The Kirsch's template is used for the detection of the blood vessels from the retinal images. The Kirsch's operator is the first order derivative which is used for edge enhancement and detection. It finds the maximum edge strength in a few preset directions. [14] For edge detection, the operator uses eight templates, which are successively rotated by 45°. The gradient is calculated by convolution of the image using eight template impulse response arrays which lie in each and every pixel. Thus, the gradient of different directions is attained. The final gradient is the summation of the enhanced edges where all directions for RGB channel is taken into consideration.

The edge magnitude of the Kirsch operator is designed as the maximum magnitude across all directions [15] such as

$$h_{n,m} = max_{z=1,2,\ldots,8} \sum_{i=-1}^{1} \sum_{j=-1}^{1} g_{ij}^{(z)} \cdot f_{n+i,\ m+j} \quad (8)$$

Where z specifies the compass direction kernels as follows:

$$g^{(1)} = \begin{bmatrix} +5 & -3 & -3 \\ +5 & 0 & -3 \\ +5 & -3 & -3 \end{bmatrix} \quad \textbf{0°}$$

$$g^{(2)} = \begin{bmatrix} -3 & -3 & -3 \\ +5 & 0 & -3 \\ +5 & +5 & -3 \end{bmatrix} \quad \textbf{45°}$$

$$g^{(3)} = \begin{bmatrix} -3 & -3 & -3 \\ -3 & 0 & -3 \\ +5 & +5 & +5 \end{bmatrix} \quad \textbf{90°}$$

$$g^{(4)} = \begin{bmatrix} -3 & -3 & -3 \\ -3 & 0 & +5 \\ -3 & +5 & +5 \end{bmatrix} \quad \textbf{135°}$$

$$g^{(5)} = \begin{bmatrix} -3 & -3 & +5 \\ -3 & 0 & +5 \\ -3 & -3 & +5 \end{bmatrix} \quad \textbf{180°}$$

$$g^{(6)} = \begin{bmatrix} -3 & +5 & +5 \\ -3 & 0 & +5 \\ -3 & -3 & -3 \end{bmatrix} \quad \textbf{225°}$$

$$g^{(7)} = \begin{bmatrix} +5 & +5 & +5 \\ -3 & 0 & -3 \\ -3 & -3 & -3 \end{bmatrix} \quad g^{(8)} = \begin{bmatrix} +5 & +5 & -3 \\ +5 & 0 & -3 \\ -3 & -3 & -3 \end{bmatrix}$$

**270°** **315°**

Fig. 1: Kirsch's Convolution Kernel

## 3. Proposed Method

The proposed algorithm can be schematically designed (shown in figure 2) for detection and segmentation of the blood vessels in retinal images:

Step 1: The color retinal fundus image is acquired from the test set of STARE database or other image banks.

Step 2: The image is then converted into Double precision.

Step 3: The image of Double class is then converted into a grayscale image.

Step 4: Adaptive Histogram Equalization is applied on the grayscale image for contrast enhancement.

Step 5: The contrast enhanced image is binarized by thresholding using Otsu algorithm.

Step 6: Morphological opening operation is carried out on the same contrast enhanced image.

Step 7: The resultant image is then subjected to Kirsch's Template operator for blood vessel extraction.

Step 8: The noise from extracted blood vessels are removed by median filtering technique.

Step 9: The output image after filtering is then subtracted from the output of step 5 to locate the hard exudates region.

Step 10: The resultant image with detected hard exudates is then compared with the detected exudates of the ground truth image.

Step 11: Finally, the performance parameters are measured to evaluate the efficiency of the proposed algorithm.

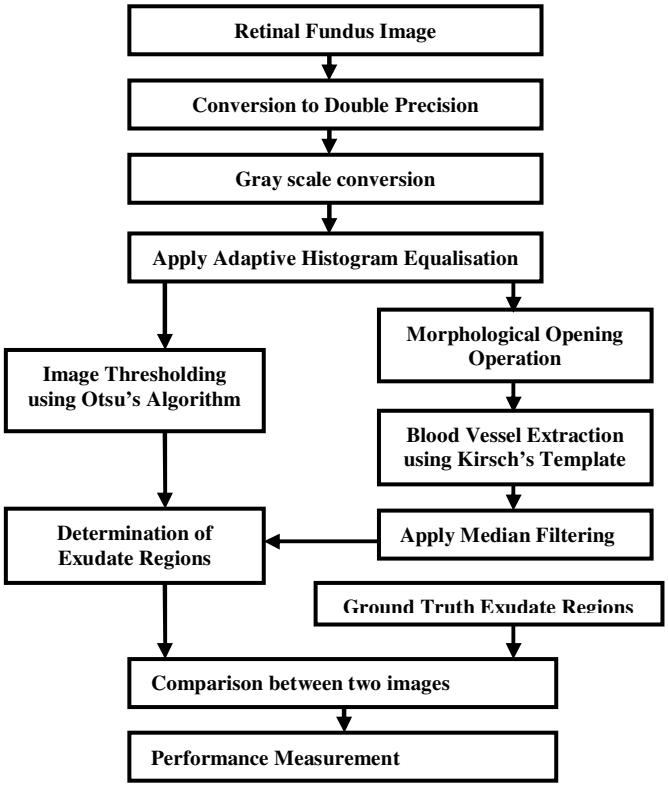


Fig. 2. Flow chart for blood vessel extraction and exudates detection

## 4. Explanation of Proposed Method

In the RGB images, the red and blue channels tend to have more noise while the green channel exhibits the best contrast between the vessels and background. Firstly, the green channel in an RGB image is converted into the double precision image before converting it in grayscale. Then, the grayscale image is contrast enhanced using Adaptive Histogram Equalization techniques to intensify the contrast of the image to provide a better transform illustration for successive image analysis steps. This technique improves the contrast adaptively across the image by restraining the maximum slope in the transformation function. This algorithm uses contrast enhancement limit, namely 'clipLimit' as 0.001, Positive integer scalar indicating the number of bins for the histogram which is used to build contrast enhancing transformation (NBins) as 128 and distributions as 'exponential' for the desired histogram shape for the image tiles [16]. The resulting image is then binarized by selecting an appropriate threshold level using Otsu's algorithm. This step helps in detecting the hard exudates from the contrast enhanced retinal fundus image.

The same contrast enhanced retinal fundus image is then undergone binary opening operator. The morphological

opening is applied using disk shaped structuring elements to enhance the vessel edges. The image after opening is then subjected to Kirsch's templates for blood vessel extraction. For edge detection, the operator uses eight templates, which are successively rotated by 45° [14]. It uses spatial filtering of the image with the help of eight templates in eight different orientations viz. 0°, 45°, 90°, 135°, 180°, 225°, 270° and 315°. The final image is calculated by summing up the gradient obtained from different directions. Thereafter, the salt and pepper noise in the image are removed by applying median filtering to the image. Then, the filtered image with extracted blood vessels is subtracted from the binarized image (obtained using Otsu's algorithm) to locate the regions where hard exudates have been formed. Finally, the detected image is compared with the ground truth exudates regions and difference performance parameters like accuracy, specificity, sensitivity, PPV, PLR and misclassified proportions are measured to assess the algorithm's efficiency.

## 5. Results

The output of the proposed algorithm for the image diagnosed with Non-Proliferative Diabetic Retinopathy (NPDR) is shown in figure 3.

We tested 15 retinal images with exudates (diagnosed with diabetic retinopathy, macular oedema, etc.) and 5 normal retinal images without exudates. They were compared to the ground-truth images obtained from reference algorithm. Table 1 shows the quantitative result of ground truth exudate numbers, detected exudate numbers, the True Positive (TP), False Positive (FP), False Negative (FN), and True Negative (TN). Based on these values, we further calculated accuracy, sensitivity, specificity, Positive Predictive Value (PPV) and the misclassified proportion of the fundus images of diseased and normal eyes which is shown in table 2.

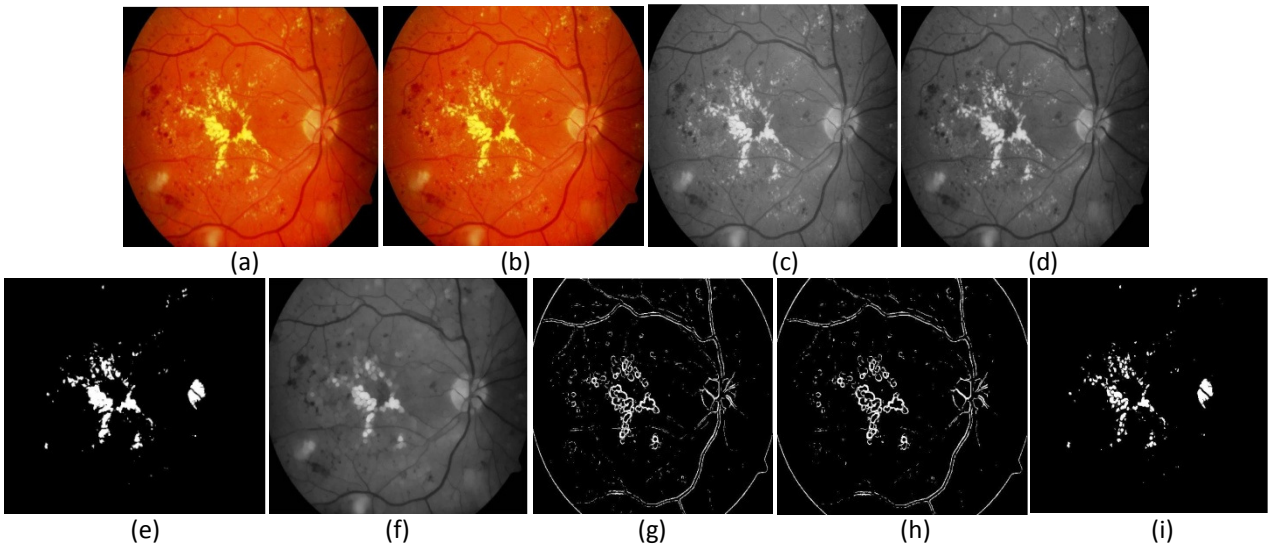


Fig. 3. (a) Original retinal fundus image in RGB, (b) Conversion into double precision, (c) Gray scale conversion, (d) Image after adaptive histogram equalisation, (e) Binarized image, obtained using Otsu's algorithm, (f) Opening on contrast enhanced image, (g) Extracted blood vessels using Kirsch's templates, (h) Noise removal using median filtering, (i) Detected hard exudates

Table 1: Pixel wise quantitative analysis of the retinal images (diseased and normal eyes both)

| SL No | Image name | Total Pixel | Ground truth Exudates Numbers | Detected Exudates Numbers | True Positive (TP) | False Positive (FP) (Detected exudate numbers - TP) | False Negative (FN) (Ground truth exudate numbers - TP) | True Negative (TN) [Total Pixel - (TP+FP+ FN)] |
|---|---|---|---|---|---|---|---|---|
| 1 | im0001 | 423500 | 14569 | 6638 | 5948 | 690 | 8621 | 408241 |
| 2 | im0050 | 423500 | 8247 | 4718 | 4048 | 670 | 4199 | 414583 |
| 3 | im0096 | 423500 | 8518 | 8688 | 6999 | 1689 | 1519 | 413293 |

| | | | | | | | | |
|---|---|---|---|---|---|---|---|---|
| 4 | im0124 | 423500 | 8803 | 4258 | 3969 | 289 | 4834 | 414408 |
| 5 | im0125 | 423500 | 8922 | 2040 | 2022 | 18 | 6900 | 414560 |
| 6 | im0140 | 423500 | 6883 | 4455 | 4057 | 398 | 2826 | 416219 |
| 7 | im0223 | 423500 | 18396 | 13727 | 11952 | 1775 | 6444 | 403329 |
| 8 | im0224 | 423500 | 36060 | 8261 | 7990 | 271 | 28070 | 387169 |
| 9 | im0225 | 423500 | 5411 | 2586 | 2375 | 211 | 3036 | 417878 |
| 10 | NPDR | 1310720 | 34469 | 27194 | 24435 | 2759 | 10034 | 1273492 |
| 11 | NPDR2 | 214000 | 3864 | 1182 | 1111 | 71 | 2753 | 210065 |
| 12 | NPDR3 | 2265025 | 56704 | 44844 | 30000 | 14844 | 26704 | 2193477 |
| 13 | NPDR4 | 1733095 | 57205 | 37751 | 33450 | 4301 | 23755 | 1671589 |
| 14 | NPDR8 | 133144 | 10628 | 4690 | 4014 | 676 | 6614 | 121840 |
| 15 | NPDR9 | 312498 | 3103 | 2335 | 2001 | 334 | 1102 | 309061 |
| 16 | NO_DR1 | 40425 | 239 | 190 | 179 | 11 | 60 | 40175 |
| 17 | NO_DR2 | 567000 | 2581 | 2042 | 1786 | 256 | 795 | 564163 |
| 18 | NO_DR3 | 165155 | 741 | 836 | 638 | 198 | 103 | 164216 |
| 19 | NO_DR4 | 1990921 | 23783 | 17596 | 16278 | 1318 | 7505 | 1965820 |
| 20 | NO_DR5 | 4898816 | 85823 | 46143 | 44401 | 1742 | 41422 | 4811251 |

Table 2: Performance analysis of the proposed algorithm on retinal images (diseased and normal eyes both)

| SL No | Image name | Accuracy (%) (TP+TN)/Total Pixel | Sensitivity (%) TP/(TP+FN) | Specificity (%) TN/(TN+FP) | PPV (%) TP / (TP+FP) | Misclassified proportion (%) (FP/Total Pixel) |
|---|---|---|---|---|---|---|
| 1 | im0001 | 97.8014 | 40.8264 | 99.8313 | 89.6053 | 0.1629 |
| 2 | im0050 | 98.8503 | 49.0845 | 99.8387 | 85.7991 | 0.1582 |
| 3 | im0096 | 99.2425 | 82.1672 | 99.5930 | 80.5594 | 0.3988 |
| 4 | im0124 | 98.7903 | 45.0869 | 99.9303 | 93.2128 | 0.0682 |
| 5 | im0125 | 98.3665 | 22.6631 | 99.9957 | 99.1176 | 0.0043 |
| 6 | im0140 | 99.2387 | 58.9423 | 99.9045 | 91.0662 | 0.0940 |
| 7 | im0223 | 98.0593 | 64.9706 | 99.5618 | 87.0693 | 0.4191 |
| 8 | im0224 | 93.3079 | 22.1575 | 99.9301 | 96.7195 | 0.0640 |
| 9 | im0225 | 99.2333 | 43.8921 | 99.9495 | 91.8407 | 0.0498 |
| 10 | NPDR | 99.0240 | 70.8898 | 99.7838 | 89.8544 | 0.2105 |
| 11 | NPDR2 | 98.6804 | 28.7526 | 99.9662 | 93.9932 | 0.0332 |
| 12 | NPDR3 | 98.1657 | 52.9063 | 99.3278 | 66.8986 | 0.6554 |
| 13 | NPDR4 | 98.3812 | 58.4739 | 99.7434 | 88.6069 | 0.2482 |
| 14 | NPDR8 | 94.5247 | 37.7682 | 99.4482 | 85.5864 | 0.5077 |
| 15 | NPDR9 | 99.5405 | 64.4860 | 99.8920 | 85.6959 | 0.1069 |
| 16 | NO_DR1 | 99.8244 | 74.8954 | 99.9726 | 94.2105 | 0.0272 |
| 17 | NO_DR2 | 99.8146 | 69.1980 | 99.9546 | 87.4633 | 0.0451 |
| 18 | NO_DR3 | 99.8177 | 86.0999 | 99.8796 | 76.3158 | 0.1199 |
| 19 | NO_DR4 | 99.5568 | 68.4438 | 99.9330 | 92.5097 | 0.0662 |
| 20 | NO_DR5 | 99.1189 | 51.7355 | 99.9638 | 96.2248 | 0.0356 |
| **AVERAGE** | | **98.4670** | **54.6720** | **99.8200** | **88.6175** | **0.1738** |

For our data set with diabetic retinopathy exudates, the average accuracy, sensitivity and specificity of the exudate detection are 98.08%, 49.54% and 99.78% respectively. The algorithm yielded high PPV (88.38%) and very low misclassified proportion (0.21%) which proves to be efficient for the algorithm.

For normal retinal image detection, the average accuracy, sensitivity and specificity are 99.63%, 70.07% and 99.94%, respectively. In addition, we got the values for PPV as 89.34% and misclassified proportion as 0.06%.

Overall, the algorithm yielded accuracy, sensitivity, specificity, PPV and misclassified proportion as 98.47%,

54.67%, 99.82%, 88.62% and 0.17% respectively (obtained by calculating the mean value of all the test results). Additionally, we measured Positive Likelihood ratio using average sensitivity and average specificity values and it calculated to be 303.73.

## 6. Conclusions and Future Scope

Retinal diseases have an adverse effect on human eye which may cause permanent blindness. Hence, early detection and diagnosis of the disease is a prime concern. The images for this algorithm have been taken from the test set of DRIVE database. The images should be of good quality in terms of sharpness, contrast, focus, etc. for proper detection and segmentation of exudates. In this present work, the thick vessels are detected by the Adaptive Histogram Equalization technique by using local thresholding in normalized images. [17] Exudates were detected using thresholding by applying the Otsu's algorithm. Kirsch's template operator is used for extracting blood vessel that has an advantage of yielding result that is more precise. The result also will be compared with the human views to get the likeliness of edge detecting against it.

The results are performance oriented and a clinical evaluation will be undertaken to integrate the presented algorithm in a tool for diagnosis of diabetic retinopathy. Our algorithm has very high accuracy which shows that the algorithm detects the exudate pixels efficiently. It also has very high specificity which proved that the algorithm does not recognize a non-exudate pixel as an exudate pixel. However, the sensitivity is relatively low value which showed that the low intensity exudates pixels are still too indefinable to be detected by this algorithm.

Hence, there are some incorrect exudate detections which are caused by the artifacts that are alike the exudates, artifacts which arrived from noise in the image acquisition process, the exudates that are adjacent to blood vessels or exudates that appear very pale. [18]
Also, in retinal images which contain severe lesions, the algorithm needs higher level thresholding and segmentation method. Hence, our future work will be to replace the simple threshold method with a more proper and result oriented approach to increase the accuracy of this method and deal with the problem of the presence of severe lesions in retinal fundus images. [19]

Further steps shall be the determining the difference between hard exudates and soft exudates, which could not be attained using the proposed algorithm. [2] However, hard and soft exudates can be distinguished by their color and the sharpness of their border so this can be achieved by tuning the edge filter and feature selection. It is anticipated that these features will be used in future detection algorithms. [11]

## References

[1] A.K. Jain, Fundamentals of digital image processing vol. 3: Prentice-Hall Englewood Cliffs, 1989.

[2] Thomas Walter, Jean-Claude Klein, Pascale Massin, Ali Erginay, ―A Contribution of Image Processing to the Diagnosis of Diabetic Retinopathy—Detection of Exudates in Color Fundus Images of the Human Retina‖, IEEE transactions on medical imaging, vol. 21, no. 10, october 2002

[3] Research Section, Digital Retinal Image for Vessel Extraction (DRIVE) Database. Utrecht, The Netherlands, Univ. Med. Center Utrecht, Image Sci. Inst. [Online]. Available: http://www.isi.uu.nl/Research/Databases/DRIVE

[4] STARE Project Website. Clemson, SC, Clemson Univ. [Online]. Available: http://www.ces.clemson.edu/~ahoover/stare/ /

[5] X. Merlin Sheeba, S. Vasanthi, ―An Efficient ELM Approach for Blood Vessel Segmentation in Retinal Images,‖ Bonfring International Journal of Man Machine Interface, Vol. 1, Special Issue, December 2011

[6] A. Hoover, V. Kouznetsova, and M. Goldbaum, ―Locating blood vessels in retinal images by piecewise threshold probing of a matched filter response,‖ IEEE Trans. Med. Imag., vol. 19, no. 3, pp. 203–210, Mar. 2000

[7] Muhammad Moazam Fraz , Paolo Remagnino, Andreas Hoppe, Bunyarit Uyyanonvara, Alicja R.Rudnicka, Christopher G. Owen, and Sarah A. Barman, ―An Ensemble Classification-Based Approach Applied to Retinal Blood Vessel Segmentation,‖ ieee transactions on biomedical engineering, vol. 59, no. 9, September 2012

[8] Shreyasi Hazra, Atashi Patra, Tuhin Utsab Paul, "A Comparative Study of Retinal Image Processing Technique for Blood Vessel Segmentation", International Journal of Science and Research (IJSR), https://www.ijsr.net/archive/v5i4/v5i4.php, Volume 5 Issue 4, April 2016, 652 - 664 doi: 10.21275/v5i4.NOV162646

[9] M. Kalaivani, M. S. Jeyalakshmi, Aparna.V, "Extraction Of Retinal Blood Vessels Using Curvelet Transform And Kirsch's Templates," International Journal of Emerging Technology and Advanced Engineering, ISSN 2250-2459, Volume 2, Issue 11, November 2012

[10] Gonzales RC, Woods RE. Digital image processing. New York: AddisonWesley; 1993. p. 75–140

[11] Akara Sopharak a, Bunyarit Uyyanonvara a, Sarah Barmanb, Thomas H. Williamson c, ―Automatic detection of diabetic retinopathy exudates from nondilated retinal images using mathematical morphology methods," Computerized Medical Imaging and Graphics Volume 32, Issue 8, December 2008, Pages 720–727

[12] Otsu, N., "A Threshold Selection Method from Gray-Level Histograms," IEEE Transactions on Systems, Man, and Cybernetics, Vol. 9, No. 1, 1979, pp. 62-66.

[13] Nobuyuki Otsu (1979). "A threshold selection method from gray-level histograms". IEEE Trans. Sys., Man., Cyber. 9 (1): 62–66. doi:10.1109/TSMC.1979.4310076

[14] Shahriar Badsha, Ahmed Wasif Reza, Kim Geok Tan, Kaharudin Dimyati, "A New Blood Vessel Extraction Technique Using Edge Enhancement and Object Classification," J Digit Imaging. 2013 Dec; 26(6): 1107–1115. PMCID: PMC3824929, Published online 2013 Mar 21, doi: 10.1007/s10278-013-9585-8

[15] Kirsch, R. (1971). "Computer determination of the constituent structure of biological images," Computers and Biomedical Research 4: 315–328. doi:10.1016/0010-4809(71)90034-6

[16] Razieh Akhavan, Karim Faez, ―A Novel Retinal Blood Vessel Segmentation Algorithm using Fuzzy 4, No. 4, August 2014, pp. 561~572 ISSN: 2088-8708

[17] Nilanjan Dey, Anamitra Bardhan Roy, Moumita Pal, Achintya Das, ―FCM based blood vessel segmentation method for retinal image‖, International Journal of Computer Science and Network (IJCSN),Volume 1, Issue 3, June 2012,ISSN 2277-5420

[18] Akara Sopharak , Bunyarit Uyyanonvara, Sarah Barman, "Automatic Exudate Detection from Nondilated Diabetic Retinopathy Retinal Images Using Fuzzy C means Clustering", Sensors 2009, 9(3), 2148-2161; doi:10.3390/s90302148

[19] R.Radha and Bijee Lakshman, "Retinal image analysis using morphological process and clustering technique", SIPIJ Vol.4, No.6, December 2013

## Author Profile:

**Shreyasi Hazra** received her B. Tech degree in Electronics and Communication Engineering from JIS College of Engineering under West Bengal University of Technology in 2012. She has worked with IBM as Application Developer for 1 year and 8 months. Currently, she is pursuing her M.Tech in Electronics and Communication from Institute of Engineering & Management under same university. Her area of interest includes image processing & analysis.

**Atashi Patra** has completed her B. Tech in Electronics and Communication Engineering from Asansol Engineering College under West Bengal University of Technology in 2013. Currently, she is pursuing her M.Tech in Electronics and Communication from Institute of Engineering & Management under same university. Her area of interest is in image processing & analysis.

**Tuhin Utsab Paul** did his undergraduate and postgraduate degrees in computer science and engineering from the University of Calcutta. He is working as an assistant professor in the department of electronics and communication at the Institute of Engineering and Management since 2012. His research area includes bio – medical image processing, digital signal processing and embedded system design.